

Synthesis, structural, morphological, optical and electrical conductivity properties of aluminium doped ZnO/POLY (*o*-TOLUIDINE) (Al-ZnO-POT) nanocomposites

N. Velmani^{a*}, D. Tamilselvi^{a,b}, K. Rathidevi^{a,c}

^{a*}Department of Chemistry, Government Arts College, Coimbatore -641 018, Tamilnadu, India

^aResearch & Development Centre, Bharathiar University, Coimbatore – 641 046, Tamilnadu, India

^bDepartment of Science and Humanities, Rathinam Technical Campus, Coimbatore – 641 021, Tamilnadu, India

^cSchool of Foundational Sciences, Department of Chemistry, Kumaraguru College of Technology, Coimbatore – 641 049, Tamilnadu, India

Aluminium doped Zinc oxide (Al-ZnO) nanoparticles synthesized by chemical precipitation method. Chemical oxidative polymerization of *o*-toluidine monomer for the synthesis of Poly (*o*-toluidine) (POT) polymer and its nanocomposites with Al-ZnO nanoparticles (Al-ZnO-POT) employing ammonium persulfate as an oxidizing agent in aqueous medium. Synthesized nanoparticles, polymer and nanocomposites were characterized with XRD studies, FTIR, SEM, EDAX, UV-Vis and PL analysis. The XRD pattern confirms an amorphous structure in Al-ZnO-POT nanocomposites. The FTIR pattern confirms functional group and chemical bonding present in the synthesized samples. SEM images confirm the nanorod shape of nanoparticles. EDAX images confirm the elemental composition of the synthesized samples. The optical property of the particles was analysed by UV-Visible and PL Spectra. Incorporation of nanoparticles, polymer and nano composites showed a significant difference in electrochemical conductivity properties were analysed by using four probe DC electrical conductivity instrument from room temperature 32°C to higher temperature 120°C.

(Received April 8, 2021; Accepted June 17, 2021)

Keywords: Al-ZnO, Poly(*o*-toluidine), Nanocomposites, Bandgap, Conductivity

1. Introduction

In the current scenario, nanocomposite materials are generally low-cost and high-performing materials due to their unique grain sizes, microstructure, high surface area, physicochemical, electrical and mechanical properties [1]. These materials have wider range of applications in various fields such as sensors, [2,3] electronic devices, [4] catalyst, [5] and energy as well as memory devices [6,7] etc. Some metal oxides (like MnO₂, ZnO, RuO₂, TiO₂, WO₃ and SnO₂) are doped with conducting polymers to form nanocomposite materials [8]. Among these all the metal oxides, ZnO nanoparticle is a nontoxic, low cost and excellent semiconductor nanomaterial with wide band gap of 3.37 eV and large excitation binding energy of 60 meV. ZnO nanoparticles are doped with different ions (such as Al, Ni, Cu, Mn, Co, Mg, etc.) to improve the electrical, optical, and catalytic properties [9-11]. Among these ions Al-doped ZnO nanoparticles are combined with Conducting polymers to form nanocomposite. Conducting polymers have created attention over the past one decade due to its unique optical and electrical properties which have significant potential commercial applications. Among such conductive polymers, polyaniline (PANI) and Poly(*o*-toluidine), (POT) have unusual conductive properties, environmentally stable, ease production, good electrochemical properties and better conductivity [12-13]. Polyaniline has provided better conductivity and environmental stability which are its main advantages but, on the

* Corresponding author: nanjanvel@gmail.com

contradictory, its insoluble nature in most organic solvents, makes it as tough in processing and Poly(*o*-toluidine), fusibility [14-16]. Poly(*o*-toluidine), (POT) is the methyl substituted polyaniline conductive polymer which has better solubility nature when compared to polyaniline. Recently PANI doped naphthalene sulphonic acid and camphor sulphonic acid synthesis was reported by the researcher using solid state polymer synthesis method. Polyaniline along with substituents ($-\text{CH}_3$, $-\text{OCH}_3$ and $-\text{OC}_2\text{O}_5$) results in better processability, polymeric network and conductivity nature [17-20]. In this paper Al-ZnO nanoparticles are synthesised by chemical precipitation method in alkaline medium, POT and Al-ZnO-POT nanocomposites are synthesised by chemical oxidative polymerization in aqueous medium. Synthesized Al-ZnO, POT and Al-ZnO-POT nanocomposites are characterized by XRD, FTIR, SEM, EDAX, UV, PL and the results of their structural, morphological, optical properties and DC conductivity studies had discussed in detail.

2. Experimental Materials and Methods

2.1. Materials

o-Toluidine, Ammonium persulphate, Zinc nitrate hexahydrate, Aluminium nitrate nonahydrate, Sodium hydroxide, Hydrochloric acid and distilled water were purchased of high purity with AR grade and used to nanocomposite preparation.

2.2. Synthesis of Al-ZnO nanoparticles

To synthesis Al-ZnO nanoparticles by chemical precipitation method the following steps were to be followed. To prepare first solution, 0.9 M of $\text{Zn}(\text{NO}_3)_2 \cdot 6\text{H}_2\text{O}$ and 0.1 M of Aluminium nitrate nonahydrate were mixed in a beaker and kept in magnetic stirrer for 10 mins under vigorous stirring. 100 ml of 2M NaOH second solution was then added in drops into the first solution under constant stirring until the pH value raises upto 12. The obtained white colour precipitate was filtered and washed with distilled water and ethanol. Then it was dried in oven at 100°C for 2hrs and as a result a white colour Al-ZnO nanoparticles formed. The dried precipitates of Al-ZnO nanoparticles are crushed into fine powder with an agate mortar. Then, the collected fine powder sample was annealed at 500°C for two hours followed by stepwise cooling at 1°C per minute and grinding to get fine particles [27].

2.3. Synthesis of POT & (Al-ZnO-POT) Nanocomposites

The following steps were involved in synthesis of Al-ZnO-POT nanocomposites by chemical oxidative polymerization method. To prepare first solution 1.10g of Al doped ZnO is dissolved in 10 ml of 1.0 mol/L HCl and the solution was added into 10.63g of *o*-toluidine monomer was dissolved in 90 ml of 1.0 mol/L HCl and then the mixture was stirred with ultrasonication to accelerate the dispersion. The second solution containing 22.82g of ammonium persulphate (APS) oxidizing agent was dissolved in 100 ml of 1.0 mol/L HCl and the second solution was then added drop-wise to the first solution under vigorous stirring in an ice bath for 8–9 hours at $0-5^\circ\text{C}$. The polymeric solution slowly starts to precipitate out. Finally, the formed precipitated polymer was washed with distilled water and ethanol, until the filtrate was colourless, dried at oven for 12 hours at 60°C . The final Al-ZnO-POT nanocomposite in base form were received by immersed in the above HCl-doped Al doped ZnO-POT nanocomposites into 400 ml of 1.0 mol/L $\text{NH}_3 \cdot \text{H}_2\text{O}$ solution under vigorous stirring for 3 hours at room temperature, followed by re-filtered, washed and dried. The dried dark green precipitates were crushed into fine powder with an agate mortar. Similar procedure was followed to synthesis of poly (*o*-toluidine) POT polymer without using of Al-ZnO nanoparticles [26].

2.4. Characterization Techniques

The structural analysis of the all synthesized samples were characterized using X-Ray Diffraction analyzer (XRD) using X'Pert PRO, X-ray diffractometer with $\text{CuK}\alpha$ radiation ($\alpha=1.5406 \text{ \AA}$). The functional group present in the samples were analyzed using Fourier Transform Infrared Spectrophotometer (FTIR), Shimadzu (Japan) in the range $4000-400 \text{ cm}^{-1}$ with pelletized KBr pellets. The surface morphology of the samples was analyzed using Scanning Electron

Microscope (SEM) with JOEL, JSM and energy dispersive EDX spectrometry. The absorbance and reflectance of the samples were analyzed using UV-reflectance spectra using UV-Visible spectrophotometer model Shimadzu UV-2100. The electrical conductivity of the synthesized Al-ZnO, POT and Al-ZnO-POT nanocomposite were predicted by using Keithley 6517B Electrometer.

3. Results and discussion

3.1. XRD studies

The XRD pattern of Al-ZnO nanoparticles, POT polymer and Al-ZnO-POT nanocomposites were presented in Fig.1. From this observed result, the characteristics of XRD sharp peaks located at $2\theta = 31.47^\circ, 35.95^\circ, 38.65^\circ, 47.25^\circ, 56.30^\circ, 62.57^\circ, 66.10^\circ, 67.66^\circ$ and 68.80° are corresponding to (100), (002), (101), (102), (110), (103), (200), (112), and (201) planes for Al-ZnO nanoparticles. The sharp peaks clearly indicate the Al-ZnO crystalline in nature, which is confirmed with JCPDS card number - 36-1451. The pure POT polymer shows a single broad peak at 2θ values around 25° , which indicates that POT polymer confirms an amorphous (or) semi crystalline structure, since there were no sharp peaks were integral factor occurred in the XRD image [21 & 22]. Al-ZnO-POT nanocomposites confirms an amorphous structure. The average crystallite size of Al-ZnO nanoparticles, POT polymer and Al-ZnO-POT nanocomposites were calculated by using following De-bye-Scherrer formula,

$$D = 0.94\lambda / \beta \cos\theta$$

where D is the average crystallite size, λ is the wavelength (1.5406 \AA), β is the Full-Width Half Maximum of Intensity and θ is the Bragg angle. The crystallite size of Al-ZnO, POT and Al-ZnO-POT are 56.32 nm, 84.90 nm and 84.89 nm respectively. When the semiconductor material was mixed with the POT the crystalline nature diminished due to the minimal amount of semiconductor material added during the synthesis of semiconductor polymeric nanocomposites which resulted in a crystalline nature. This was observed with the considerable change in the XRD image of the polymeric nanocomposites. These XRD results justified the incorporation of semiconductor material into the polymeric chain would result in enhanced conductivity [18-19].

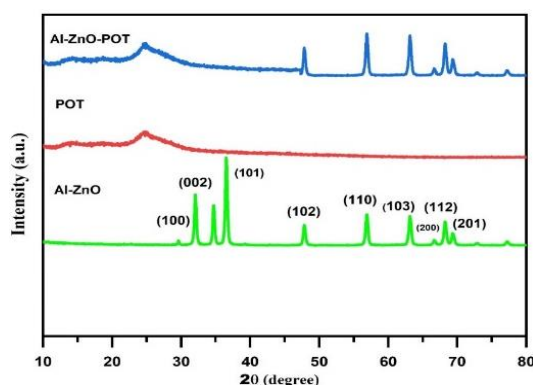


Fig. 1. XRD patterns of Al-ZnO, POT and Al-ZnO-POT.

3.2. FTIR - (Fourier transform infra-Red Spectroscopy) - Analysis

The FTIR analysis of Al-ZnO nanoparticles, POT polymer and Al-ZnO-POT nanocomposites were presented in Fig.2. The formation of Al-ZnO nanoparticles showed peaks at 3453 cm^{-1} and 1645 cm^{-1} corresponding to O-H stretching and bending vibrations of water molecules and the peaks at 1378 cm^{-1} corresponding to the presence of NO_3^- was confirmed. A peak around 529 cm^{-1} corresponding to the formation of Zn-O metal oxide bond [(3-6)]. The formation of POT polymer showed a peak at 2921 cm^{-1} corresponding to the C-H stretching of the methyl

group. The peaks at 1603 cm^{-1} and 1493 cm^{-1} corresponding to C=C stretching vibration of quinoid and benzenoid rings in POT polymeric chain. The peaks at 1382 cm^{-1} and 3459 cm^{-1} corresponding to C-N and N-H stretching vibration linked to benzenoid rings in POT polymeric chain. The peaks at 1156 cm^{-1} and 810 cm^{-1} corresponding to C-H plane stretching vibration of quinoid rings and C-H out plane bending vibration of benzenoid rings. The formation of Al-ZnO-POT nanocomposites showed an absorption peaks are centered at around 3459 , 1634 , 1371 and 527 cm^{-1} respectively [23]. Comparing to that of pure POT polymer, the absorption peaks of Al-ZnO-POT nanocomposites have been shifted to lower wave numbers, the shift of absorption peaks may be corresponding to the formation of hydrogen bonding between Al-ZnO and the -NH group of POT polymer on the surface of the Al-ZnO nanoparticles. In case of Zn-O nanoparticles a peak at around 529 cm^{-1} corresponding to Zn-O stretching was observed but changes found in Al-ZnO-POT nanocomposites because of the presence of interactions between POT and Al-ZnO nanoparticles. These results suggest that Al-ZnO nanoparticles were effectively covered by POT. The main reason for the incorporation of the semiconductor material into the polymeric lattice is to improve the conductivity and thereby increasing the free flow of electrons in the polymeric chain. The secondary amine present in the polymeric chain also plays a significant role in the conductivity due to the presence of lone pair of electrons present on the polymeric backbone [24].

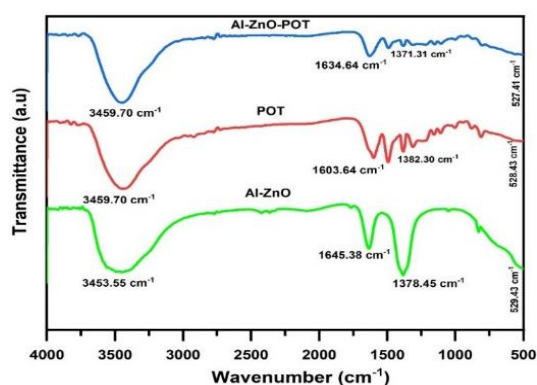


Fig. 2. FTIR patterns of Al-ZnO, POT and Al-ZnO-POT.

3.3. SEM Analysis

The surface morphological nature of the Al-ZnO, POT and Al-ZnO-POT nanocomposites were analysed using SEM studies and presented in the Fig.3. Al-ZnO nanoparticles shows that uniform distribution of nanorod shape and crystalline structure. POT shows that small sheet like amorphous (or) semi crystalline structure with irregular agglomerations, which connected with each other. When compared with pure Al-ZnO and POT polymer, Al-ZnO-POT nanocomposites shows that cluster of porous material due to the attachment of Al-ZnO nanoparticles [24-27].

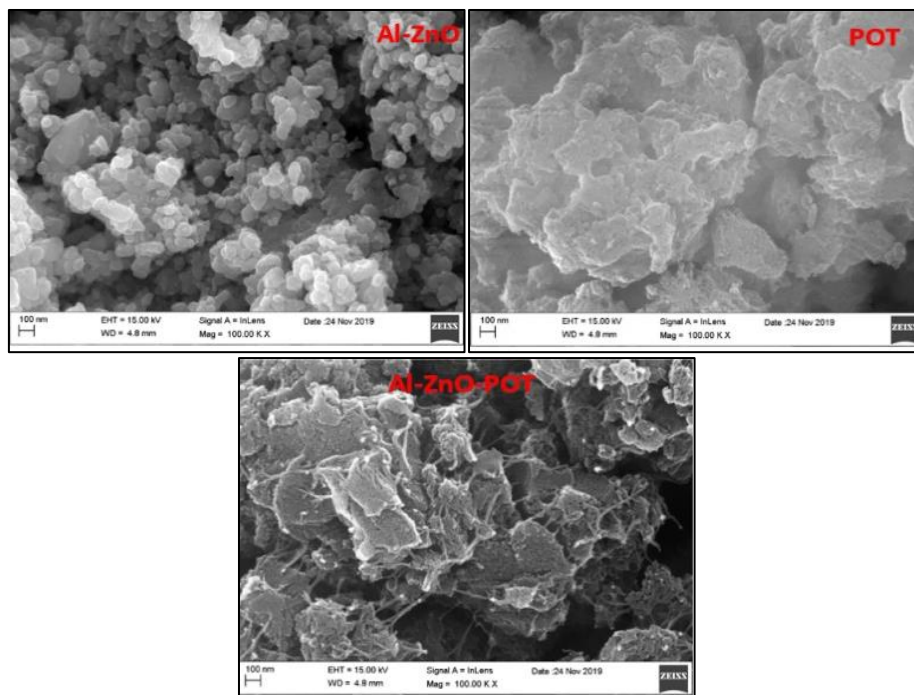


Fig. 3. SEM images of Al-ZnO, POT and Al-ZnO-POT.

3.4. EDAX Analysis

The chemical composition of the Al-ZnO, POT and Al-ZnO-POT nanocomposites were further investigated by EDAX Analysis which presented in the Fig.4. From the figure, the presence of the Zn, O, Al, C and N elements were confirmed. EDAX graph shows that no impurities present in the synthesized pure Al-ZnO, POT and Al-ZnO-POT nanocomposites.

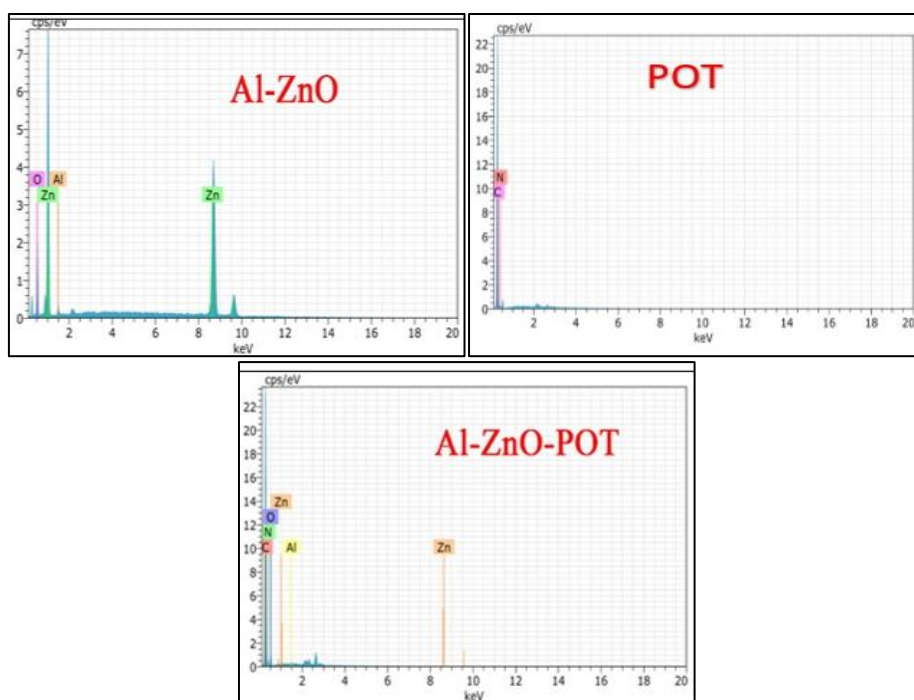


Fig. 4. EDAX images of Al-ZnO, POT and Al-ZnO-POT.

3.5. UV-Visible analysis

The optical properties of Al-ZnO, POT and Al-ZnO-POT nanocomposites were analyzed by using UV-Visible spectral studies and the result was shown in Fig.5. The UV-Visible spectra of Al-ZnO shows that the absorption peak appears at around 364 nm. Which is the single characteristic absorption peak of pure Al-ZnO nanoparticles. From figure POT shows that two characteristic absorption peaks at around 303 nm and 550 nm. The peak at 303 nm corresponded to the π - π^* transition of the benzenoid rings, while the peak at 550 nm is attributed to n- π^* transition of benzenoid to quinoid rings. Al-ZnO-POT nano composites, which is similar to pure POT and absorption peaks were slight blue shift to around 298 nm and 510 nm respectively and the intensity of absorption peaks increased. The wavelength decreased may be attributable to the interaction between Al-ZnO and POT, which cause easy charge transfer from POT to Al-ZnO nanoparticles via hydrogen bonding.[20].

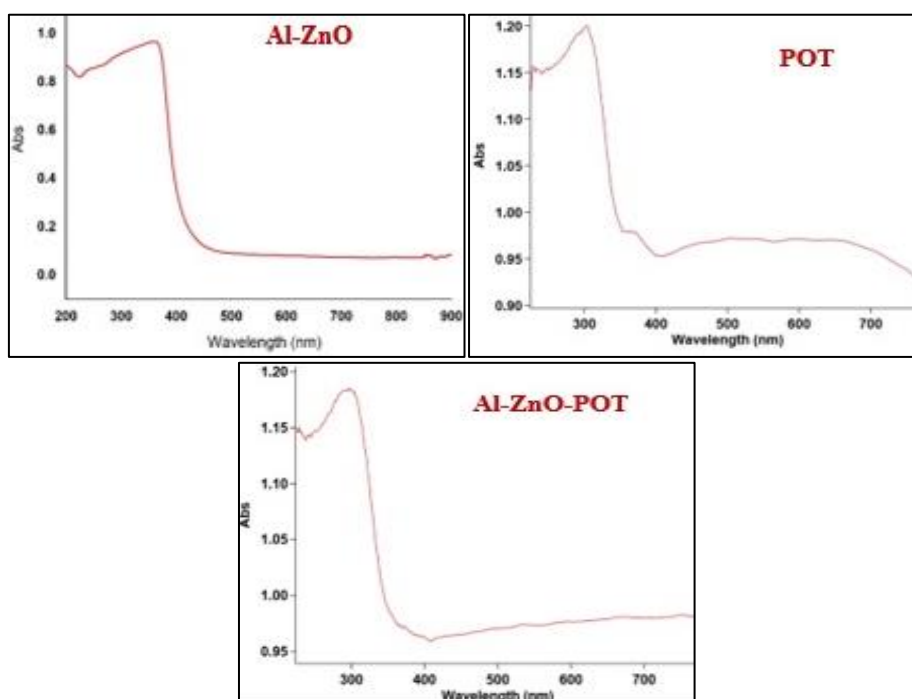


Fig. 5. UV-Visible pattern of Al-ZnO, POT and Al-ZnO-POT.

3.6. Band-gap Calculation

The optical band gap value E_g of Al-ZnO, POT and Al-ZnO-POT was obtained by using the modified Kubelka-Munk (K-M) function $[F(R)hv]^2$ versus photon energy (eV) ($[F(R)hv]^2 = \{(1-R)^2/2R\} * hv^2$) and the result was shown in Fig.6. The optical band gap value E_g of the Al-ZnO, POT and Al-ZnO POT samples exhibited as 3.20 eV, 3.27 eV and 3.30 eV for respectively [6,27&28].

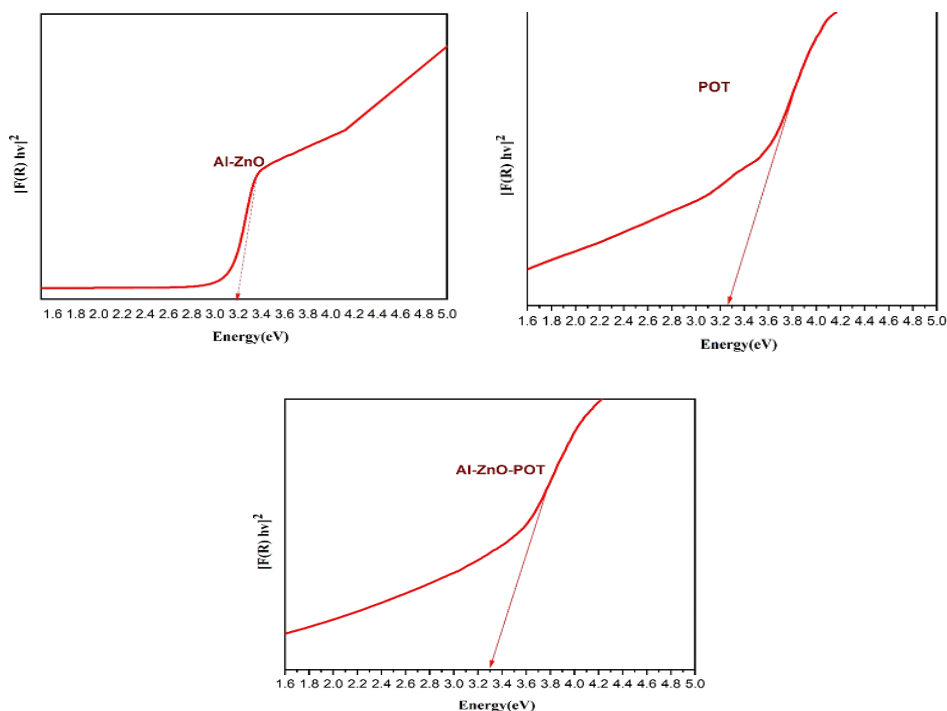


Fig. 6. Band-gapplot of Al-ZnO, POT and Al-ZnO-POT.

3.6. PL Spectral Analysis

The PL spectra of synthesized Al-ZnO nanoparticles, POT and Al-ZnO-POT nanocomposites were shown in Fig.7. From figure Al-ZnO nanoparticles shows that at different excitation wavelengths of 292 nm and 466 nm. POT shows that at different excitation wavelengths of 294 nm and 362 nm. Al-ZnO-POT shows that at different excitation wavelengths of 294 nm and 361 nm. From the observations, it was noted that the PL intensity of each sample was strongly enhanced after Al-ZnO doped with POT. The intensity of UV emission was found to decrease as Al-ZnO doped with POT, which may be due to their density of free exciton [20 & 24].

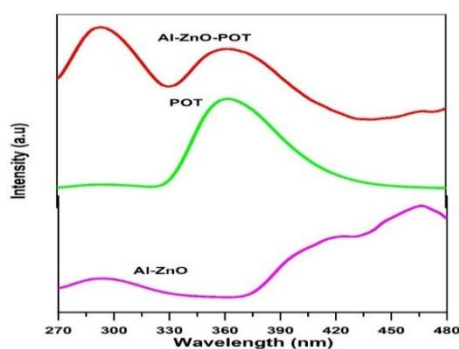


Fig. 7. PL pattern of Al-ZnO, POT and Al-ZnO-POT.

3.7. Electrical conductivity Properties

The electrical conductivity properties of synthesized Al-ZnO nanoparticles, POT and Al-ZnO-POT nanocomposites against difference in temperature is presented in Fig.8. The 250mg of Al-ZnO, POT and Al-ZnO-POT nano composites were finely grained by Mortar Pestle and 3mm sized pellets were made at room temperature with the help of hydraulic pressure instrument. The

pressed pellets were studied by using four-probed electrical conductivity measuring technique. The electrical conductivity properties were measured by using Ohm's law, $V = RI$ where, I is the current (in Amperes) through a resistor R (in ohms) and V is the drop-in potential (in volts) across it. The reciprocal of resistance (R^{-1}) is called conductance, the flow of current I as a result of gradient in potential leads to energy being dissipated (RI^2 joule s^{-1}). In Ohmic material, the resistivity measured is proportional to the sample cross-section A and inversely proportional to its length l : $R = \rho l / A$ where ρ is the resistivity measured in Ω cm. Its inverse $\sigma = \rho^{-1}$ is the conductivity. From figure shows that there is an increase in current due to increase in temperature at all the level of voltages. A similar behavior was also observed at the temperature dependence of DC conductivity was increased with increase of temperatures which is indicating a semiconductor behavior for all the synthesized samples of Al-ZnO nanoparticles, POT polymer and Al-ZnO-POT nanocomposites. As a result, the conductance of the Al-ZnO-POT nanocomposites showed enhanced electrical conductance compared to Al-ZnO nanoparticles and POT conducting polymer, due to the addition of aluminium doped zinc ion into the polymeric lattice resulted in the enhanced conductivity. This steady increase in the electrical conductance was due to the presence of lone pair of electrons present in the secondary amine of the polymeric backbone and the electropositive dopants atoms. These electrons will flow freely along the band edge position thus resulting in the gradual increase in the electrical conductance [23&24]. This was evident from Fig. 8.

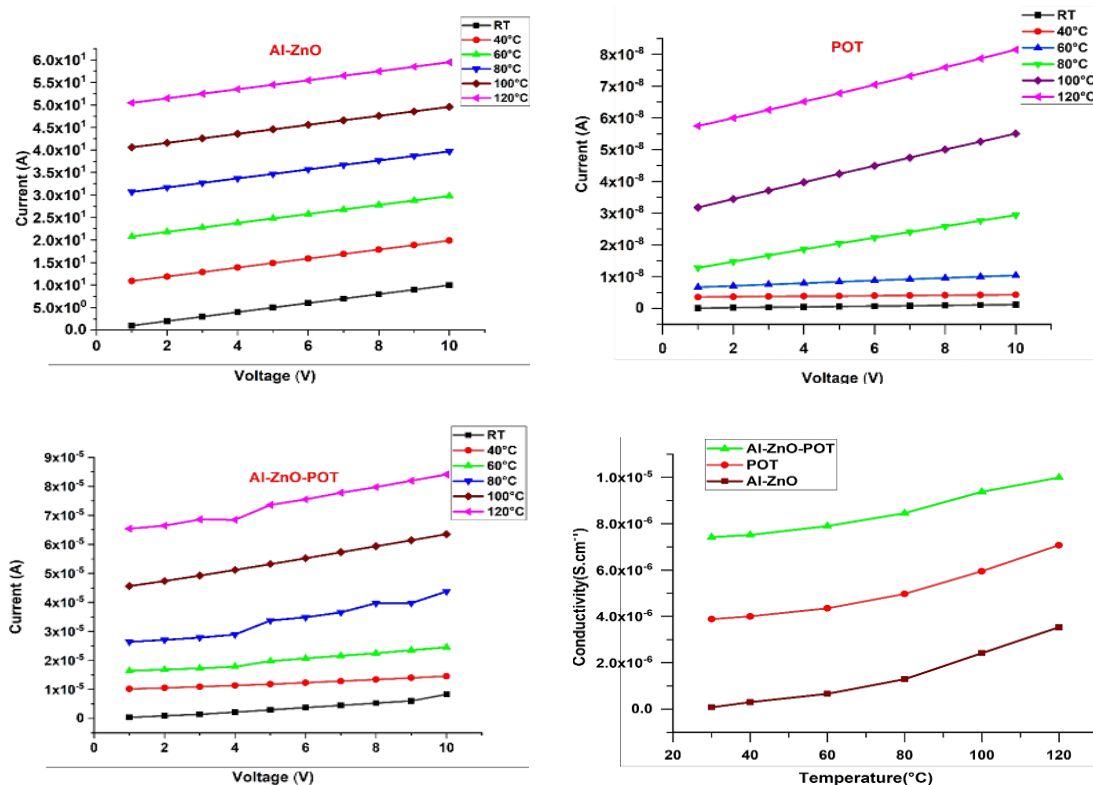


Fig. 8. Electrical conductivity properties of Al-ZnO, POT and Al-ZnO-POT.

4. Conclusion

Al-ZnO nanoparticles were synthesized using chemical precipitation method in alkaline medium. Poly(*o*-toluidine) (POT) conducting polymer and Aluminium doped zinc oxide Poly(*o*-toluidine) (Al-ZnO-POT) nanocomposites were synthesized using chemical oxidative polymerization reaction using ammonium persulphate (APS) as oxidizing reagent in acidic medium. The spectral characterization results justified the formation of the nanoparticles, polymer and nanocomposites. The XRD images confirmed the formation of Al-ZnO with sharp peaks and

addition of POT polymer resulted in the broad peaks. SEM image of Al-ZnO-POT nanocomposites shows that cluster of porous material due to the attachment of Al-ZnO nanoparticles. The functional groups and bonding of Al-ZnO-POT nanocomposites were identified from FT-IR spectra. The UV studies showed a peak at 550 nm corresponding to the substituted poly(*o*-toluidine). Increase in electrical conductance with increase in temperature was observed. Temperature plays a pivotal role in increasing the thermal conductance of the nanocomposites material. Upon comparison, the electrical conductance of the Aluminium doped zinc oxide Poly(*o*-toluidine) nanocomposites showed enhanced electrical conductance with increase in temperature was observed, due to the presence of dopant along with the lone pair of electrons present in the polymeric backbone.

References

- [1] R. M. Mohsen, S. M. Morsi, M. M. Selim, A. M. Ghoneim, H. M. El-Sherif, *Polym. Bull.* **76**, 1 (2019).
- [2] N. Pande, D. Jaspal, A. Malviya, A. Warke, *Nano-Metal Chem.* **47**(7), 999 (2017).
- [3] N. S. Pande, D. Jaspal, A. Warke, V. V. Chabukswar, *Polym. Res. J.* **10**(4), 239 (2016).
- [4] S. A. Kumar, J. S. Shankar, B. K. Periyasamy, S. K. Nayak, *Polym. Plast. Technol. Mat.* **58**(15), 1597 (2019).
- [5] K. N. Handore, S. V. Bhavsar, N. Pande, P. K. Chhattise, S. B. Sharma, S. Dallavalle, V. Gaikwad, K. C. Mohite, V. V. Chabukswar, *Polym. Plast. Technol. Eng.* **53**(7), 734 (2014).
- [6] A. Kaushar, *Polym. Plast. Technol. Mat.* **59**(7), 765 (2020).
- [7] S. S. Nejad, M. Rezaei, M. Bagheri, *Polym. Plast. Technol. Mat* **59**(14), 398 (2020).
- [8] S. Vyas, S. Shivhare, A. Shukla, **4**(7), 86 (2017).
- [9] J. N. Hasnidawani, H. N. Azlina, H. Norita, N. N. Bonnia, S. Ratim, E. S. Ali, **19**, 211 (2016).
- [10] V. R. Venu Gopal, Susmita Kamila, *ApplNanosci.* **7**, 75 (2017).
- [11] Debadrito Das, Animesh Kumar Datta, Divya Vishambhar Kumbhakar, Bapi Ghosh, Ankita Pramanik, Sutha Gupta **9**, 26 (2017).
- [12] Shama Islam, Mohsin Ganaie, Shabir Ahmad, M. Siddiqui Azher, M. Zulfequar, *International Journal of Physics and Astronomy* **2**, 105 (2014).
- [13] M. Shakir, M. S. Khan, S. I. Al-Resayes, U. Baig, P. Alam, R. H. Khan, M. Alam, *Royal Society of Chemistry Adv.* (2014).
- [14] Mohhamed Kashif, Sharif Ahmad, *Royal Society of Chemistry Adv.* **4**, 20984 (2014).
- [15] Salma Bilala, Shehna Farooqa, Anwar-ulHaq Ali Shahb, Rudolf Holzec, *Synthetic Metals* **197**, 144 (2014).
- [16] Asif Ali Khan, Shakeeba Shaheen, *Royal Society of Chemistry Adv.* **7**, 2077 (2015).
- [17] J. Liu, Z. P. Wen, X. H. Liu, Y. Tan, S. Y. Yang, P. Zhang, *Colloid. Polym. Sci.* **293**, 1391 (2015).
- [18] R. K. Fakher Alfahed, K. I. Ajeel, *International Journal of Materials Science and Engineering* **3**, 4 (2015).
- [19] Jiwei Huang, Chuanbo Hu, Yongquan Qing, *Int. J. Electrochem. Sci.* **10**, 10607 (2015).
- [20] Chuanbo Hu, Ying Li, Yazhou Kong, Yushi Ding, *Synthetic Metals* **214**, 62 (2016).
- [21] Shama Islam, Hana Khan, Zubair MSH Khan, Shabir Ahmad Kumar, Raja Saifu Rahman, M. Zulfequara, *American Institute of Physics* **1953**, 130028 (2018).
- [22] Anand Kumar, Vazid Ali, Sushil Kumar, M. Husain, *International Journal of Polymer Analysis and Characterization* **16**, 298 (2011).
- [23] Seema Joon, Rakesh Kumar, Avani Pratap Singh, Rajni Shukla, S. K. Dhawan, *Royal Society of Chemistry Adv.* **5**, 55059 (2015).
- [24] D Tamilselvi, N Velmani, K Rathidevi., *Egyptian Journal of Chemistry* **62**(6), pp. 785 - 795 (2019).
- [25] S. Satheeskumar, V. Jeevanantham, D. Tamilselvi, *Journal of Ovonic Research* **14**, 9 (2018).
- [26] D. Tamilselvi, N. Velmani, K. Rathidevi, *Mediterranean Journal of Chemistry* **9**(5),

- 403 (2019).
- [27] D. Tamilselvi, N. Velmani, K. Rathidevi, *Journal of Ovonic Research* **16**, 123 (2020).
- [28] K. Rathidevi, N. Velmani, D. Tamilselvi, *Journal of Ovonic Research* **16**, 337 (2020).
- [29] R. Anitha, E. Kumar, K. Rathnakumar, S. C. Vella Durai, *Journal of Ovonic Research* **17**, 99 (2021).
- [30] S. C. Vella Durai, E. Kumar, Indira, D. Muthuraj, *Journal of Ovonic Research* **16**, 345 (2020).